Supporting Information

A hollow MnO_2 nanozymes empowered injectable hydrogel for intrauterine adhesions therapy by alleviating oxidative stress and promoting endometrial repair

Ying Xu,†[a] Zi Ye,†[a,b] Sentao Hu,[a,b] Lichao Chu,[a] Liaobing Xin,*[b] Wangyan He,[a] Weijun Tong,*[a] Songying Zhang,*[b] Lie Ma*[a,b]

[a] MOE Key Laboratory of Macromolecular Synthesis and Functionalization, Department of Polymer Science and Engineering, Zhejiang University, Hangzhou 310058, China

[b] Key Laboratory of Reproductive Dysfunction Management of Zhejiang Province, Assisted Reproduction Unit, Department of Obstetrics and Gynecology, Sir Run Run Shaw Hospital, School of Medicine, Zhejiang University, Hangzhou 310016, China

[1] These authors contributed equally.

*Corresponding authors: liema@zju.edu.cn; zhangsongying@zju.edu.cn; tongwj@zju.edu.cn; xlbing01@163.com

1. Experimental section

1.1. Materials

Tetraethyl orthosilicate (TEOS) was purchased from Thermo Scientific (USA). Hydroxypropyl cellulose (Mw = 100 kDa） was purchased from Rhawn (Shanghai, China). Sodium hyaluronate (HA, Mw = 100 kDa) was purchased from Harvers Biotech Co., Ltd (Jiangsu, China). 4-(4,6-dimethoxy-1,3,5-triazine-2-yl)-4-methylmorpholinium chloride (DMTMM) and E2 were purchased from Aladdin (Shanghai, China). Tetrabutylammonium hydroxide (TBA-OH), 1H-benzotriazol-1-yloxytris(dimethylamino)phosphonium hexafluorophosphate (BOP), and 5-methylfurfurylamine were purchased from TCI (Japan). Other materials were purchased from Sinopharm Chemical Reagent Co., Ltd (Shanghai, China).

1.2. Synthesis of MnO_2 and MnO_2@E2 NPs

SiO_2 was synthesized as followed. Briefly, 25 mL ethanol, 1 mL water and 3 mL ammonium hydroxide were mixed at 55 °C for 10 min and dropped in the solution of 3 mL TEOS and 25 mL ethanol, followed with addition of 3 mL ammonium hydroxide 10 min later. The mixture reacted at 55 °C for 90 min, and the product was washed and dispersed in the water. 0.05g as-prepared SiO_2, 0.005 g hydroxypropyl cellulose and 180 μL ethanol were dispersed in 12 mL water in which $KMnO_4$ was added and heated at 85 °C for 2 h under reflux condition. MnO_2-coated SiO_2 NPs were resuspended in 2 M Na_2CO_3 at 60 °C for 8 h to obtain hollow MnO_2 NPs. Finally, 1.5 mg MnO_2 NPs were dispersed in 6 mL water, and different amount of E2 in 100 μL THF was added to the solution. After stirring at 25 °C for 24 h, MnO_2@E2 NPs were synthesized.

1.3. Characterizations of MnO_2 and MnO_2@E2 NPs

Transmission electron microscopy (TEM, HT7800, Hitachi, Japan) and scanning electron microscopy (SEM, SU8010, Hitachi, Japan) were employed to characterize the microstructure of NPs. The composition and structure of the NPs were analyzed by X-ray photoelectron spectroscopy (XPS, K-Alpha, Thermo Scientific, USA), X-ray diffraction (XRD, XRD-6000, Shimadzu, Japan), and infrared spectroscopy (FT-IR, Tensor II, Bruker, Germany). The nitrogen adsorption-desorption isotherm was measured using an automatic surface area and pore size analyzer (Autosorb-iQ, Quantachrome, USA). The particle size and potential were characterized by a nanoparticle analyzer (ZCEC, Malvern Panalytical, UK).

Drug loading and release properties: E2 loaded in MnO_2@E2 NPs was extracted by THF, and its mass was calculated through the absorbance at 281 nm measured by Ultraviolet-Visible spectrophotometer (UV-Vis, UH5300, Hitachi, Japan). For the measurement of drug release property, suspension of 20 mg MnO_2@E2 NPs was added to dialysis bag (Mw = 8–14 kDa), which was immersed in another 22 mL PBS (pH = 7.4, 0.1% Tween 80), and incubated at 37 °C for 120 r. At specific time points, leachate was extracted as the sample. The absorbance of the leachate at 283 nm was measured.

ROS scavenging properties: The H_2O_2 removal ability of NPs was tested as followed. NPs and H_2O_2 (100 μM) were incubated at 37 °C for 30 min. After centrifugation, the supernatant reacted with KI (1 M) solution for 5 min, and the absorption at 350 nm was recorded. The $\bullet O_2^-$ inhibition ability was detected using Total Superoxide Dismutase Assay Kit with WST-8 (Beyotime, Shanghai, China).

1.4. Preparation of HA-A and HA-F

Briefly, 1 wt% sodium hyaluronate solution in water was prepared and Dowex 50WX8 ion-exchange resin was added. After being stirred and filtered, the solution was neutralized with TBA-OH. After lyophilization, 0.5 g outcome, 0.205 g N-(2-aminoethyl) maleimide trifluoroacetate and 0.357 g BOP reacted in 20 mL anhydrous dimethyl sulfoxide under a nitrogen atmosphere for 3 h at room temperature. The product was dialyzed and freeze-dried to yield HA-A. In addition, 2 g sodium hyaluronate was dissolved in 200 mL MES buffer (0.1 M) and 5.65 g DMTMM was added. After stirring for 10 min, the mixture reacted with 1.12 mL 5-methylfurfurylamine for 24 h. After filtration, the solution was dialyzed and lyophilized to obtain HA-F.

1.5. Swelling property of HME hydrogel

The hydrogel samples were immersed in PBS (pH = 7.4), incubating at 37 °C for 48 h. The mass of the hydrogels after swelling equilibrium (W_s) and following with drying (W_d) were weighed. The swelling ratio (SR) was calculated by the equation: SR = $(W_s - W_d)/W_d \times 100$ %.

1.6. *In vivo* biocompatibility of HME hydrogel

SD rats with the treatment of HME were euthanized at 45 d after the operation. Major organs were collected and subjected to H&E staining for organ histology. Healthy untreated rats were employed as the control group.

1.7. *In vitro* degradation properties of HME hydrogel

Degradation behavior: Hydrogels, whose initial dry weight were designated as

W_0, were immersed in 200 U/mL hyaluronidase in PBS (pH = 7.4) at 37 °C. They were freeze-dried and weighed as W at specific time points, and calculated by the formula: Remaining mass = W/W_0 × 100 %.

Degradation properties of MnO_2@E2 NPs: HME hydrogel was added to the dialysis tube (Mw = 8–14 kDa), which was immersed in the medium and incubated at 37 °C at 120 r. The leaching solution was extracted at specific time points and the concentration of Mn^{2+} was detected by inductively coupled plasma-mass spectrometry (ICP-MS, Agilent, USA).

1.8. *In vivo* degradation property of HME hydrogel

At different time points, the experimental SD rats were euthanized and remaining hydrogels in the uterine tissues were collected and weighed (W), and the initial weight of hydrogel was set as W_0, which was calculated by the equation: Remaining mass = W/W_0 × 100 %.

Table S1. Primer sequences for qPCR in cellular experiments.

Primer name	Forward primer sequence	Reverse primer sequence
TNF-α	GACTCAAATGGGCTTTCCGA	TCCAGCCTCATTCTGAGACAGAG
IL-1β	CTGTGACTCATGGGATGATGATG	CGGAGCCTGTAGTGCAGTTG
IL-6	TAGTCCTTCCTACCCCAATTTCC	TTGGTCCTTAGCCACTCCTTC
CD206	CTCTGTTCAGCTATTGGACGC	TGGCACTCCCAAACATAATTTGA
CD86	TGTTTCCGTGGAGACGCAAG	TTGAGCCTTTGTAAATGGGCA
IL-10	GGTTGCCAAGCCTTATCGGA	TTCAGCTTCTCACCCAGGGA
IL-4	ATCCTGCTCTTCTTTCTCGAATGT	GCCGATGATCTCTCTCAAGTGATT
β-actin	GGCTGTATTCCCCTCCATCG	CCAGTTGGTAACAATGCCATGT

Table S2. Primer sequences for RT-qPCR in animal experiments.

Primer name	Forward primer sequence	Reverse primer sequence
IL-6	TAAGGACCAAGACCATCCAACT	TGCCGAGTAGACCTCATAGTG
IL-1β	CTCATTGTGGCTGTGGAGAAG	ACACTAGCAGGTCGTCATCAT
TNF-α	ATGTGGAACTGGCAGAGGAG	ACGAGCAGGAATGAGAAGAGG
IL-10	CAGACCCACATGCTCCGAGA	CAAGGCTTGGCAACCCAAGTA
IL-4	ACAAGGAACACCACGGAGAA	TTCAAGCACGGAGGTACATCA
VEGF	GCCTTGTTCAGAGCGGAGA	CGCCTTGGCTTGTCACATC

Table S3. Statistical table of pregnancy rates and embryo implantation ratios in different groups.

Groups	Number of pregnant rats in left uteri	Number of pregnant rats in right uteri	Pregnancy rate in right uteri (%)	Number of embryos in left uteri	Number of embryos in right uteri	Relative embryos implantation (%)
NR	11	1	9.1	79	9	11.4
H	10	1	10.0	63	5	7.9
HM	10	4	40.0	70	15	21.4
HME	11	5	45.5	88	27	30.7[a, b]

a: $p < 0.05$, NR versus HME

b: $p < 0.01$, H versus HME

Table S4. Statistics on abortions in rat fertility test.

Groups	Number of rats with abortions in right uteri	Number of pregnant rats including abortions in right uteri	Abortion rate in right uteri (%)	Number of abortions and embryos in left uteri	Number of abortions and embryos in right uteri
NR	1	2	50.0	4/79	2/9
H	1	2	50.0	2/63	1/5
HM	2	4	50.0	2/70	5/15
HME	2	5	40.0	0/88	7/27

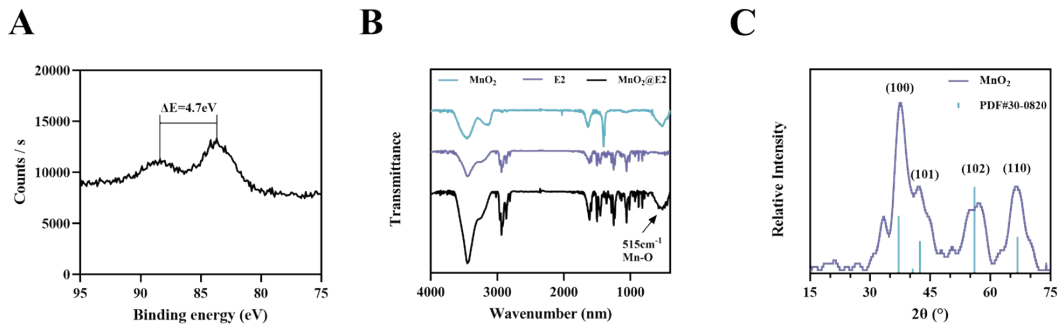

Fig. S1. (A) XPS spectrum of Mn3s of MnO_2 NPs. (B) IR spectra of MnO_2, E2 and MnO_2@E2. (C) XRD analysis of MnO_2 compared with standard PDF#30-0820 (MnO_2).

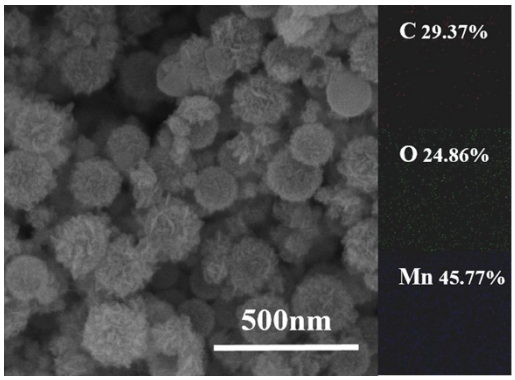

Fig. S2. SEM and EDS elemental mapping images of MnO_2@E2 NPs.

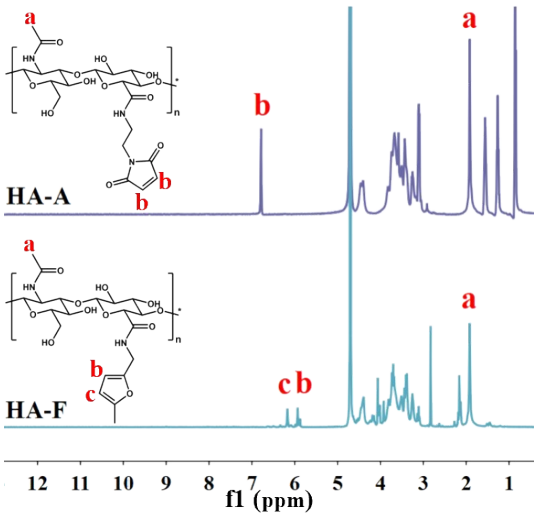

Fig. S3. [1]H NMR spectrum of HA-A and HA-F.

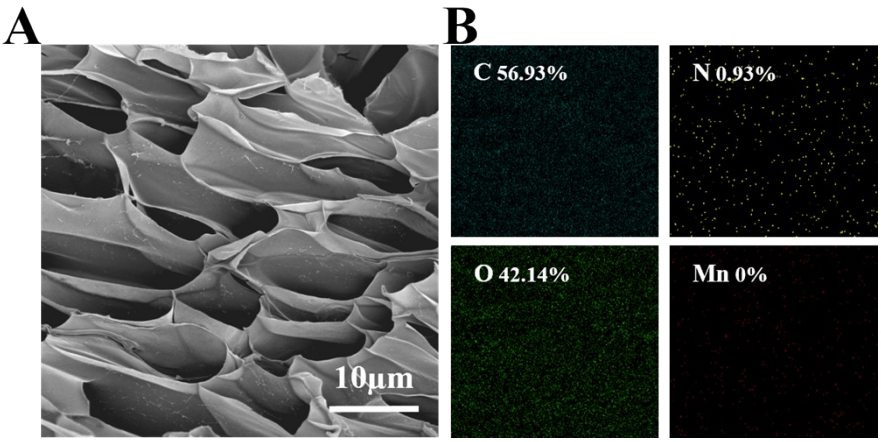

Fig. S4. SEM and EDS elemental mapping images of the H hydrogel.

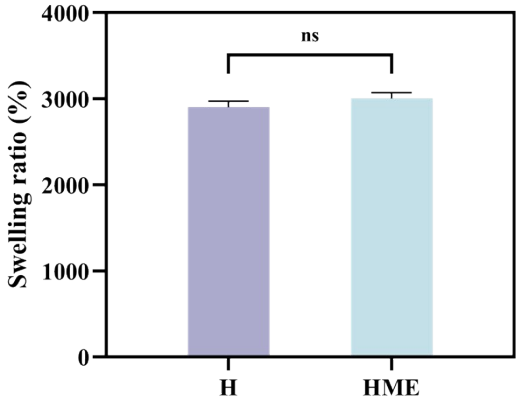

Fig. S5. Swelling ratios of hydrogels (n = 3).

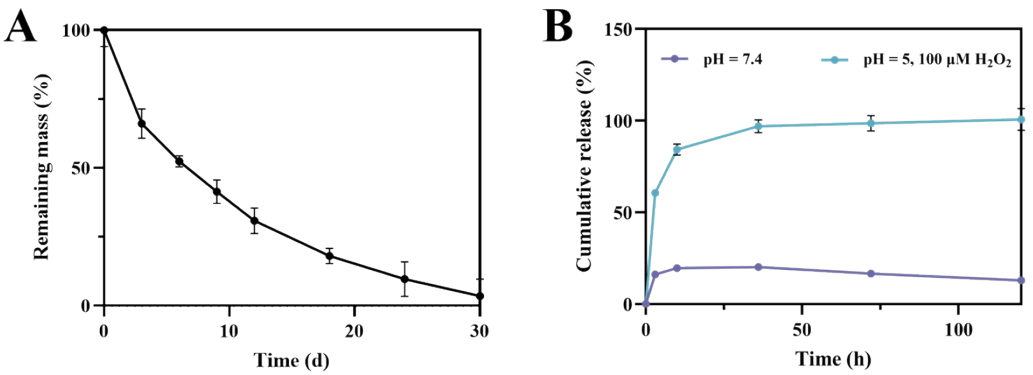

Fig. S6. *In vitro* degradation properties of HME. (A) Remaining mass curve of HME (n = 3). (B) Mn^{2+} release properties from the HME hydrogel in different environments (n = 3).

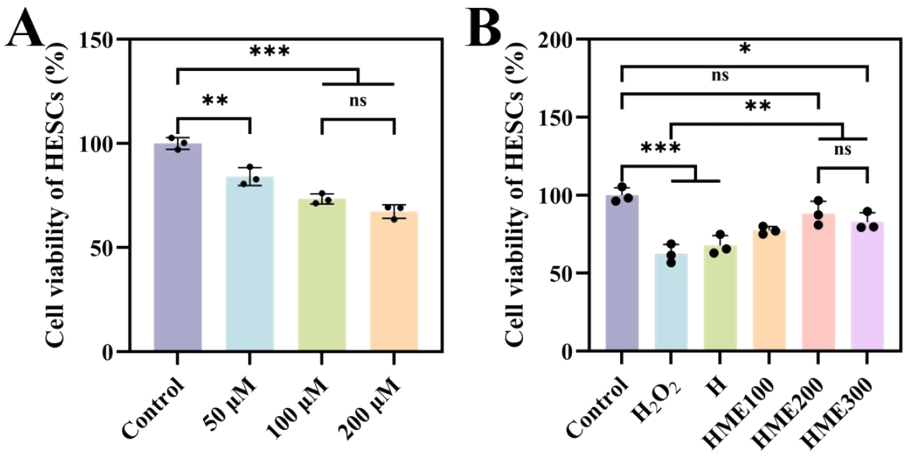

Fig. S7. (A) Cell viability of HESCs under different H_2O_2 concentrations (n = 3). (B) Cell viability of HESCs with different treatments under H_2O_2 condition (n = 3).

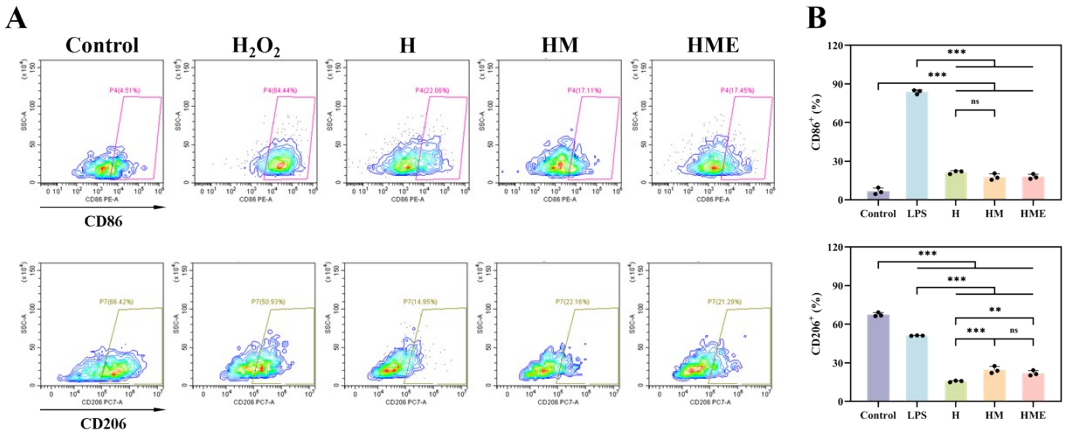

Fig. S8. (A) Representative flow cytometry plots of CD86 and CD206 positive cells (%) of BMDMs cultured with the hydrogels and (B) quantitative analysis (n = 3).

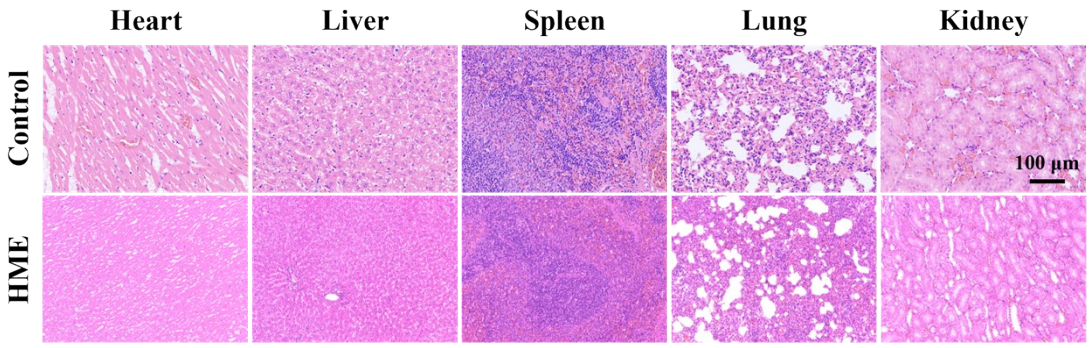

Fig. S9. *In vivo* biocompatibility assessment of HME hydrogel to major organs (heart, liver, spleen, lung and kidney) by H&E staining at 14 days after different treatments.

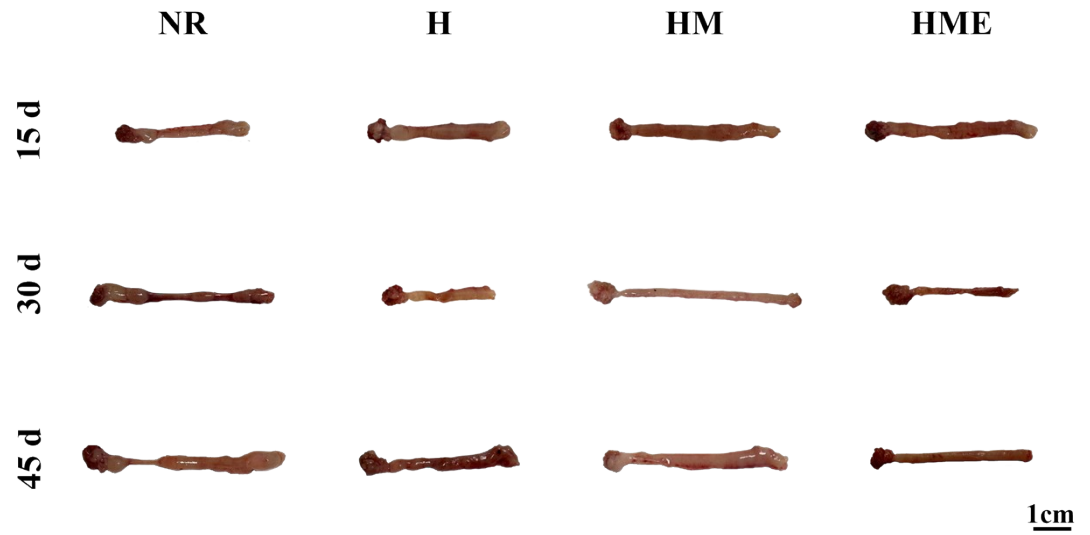

Fig. S10. Morphology of uteri at 15 d, 30 d, and 45 d after different treatments.

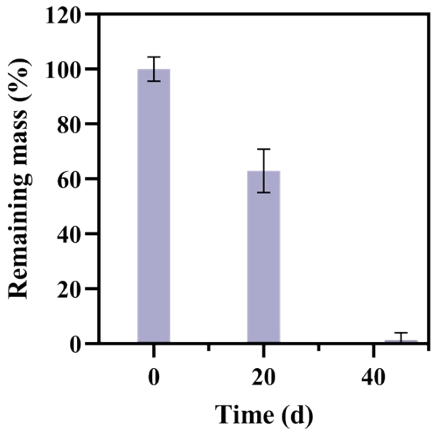

Fig. S11. *In vivo* degradation profile of HME (n = 4).

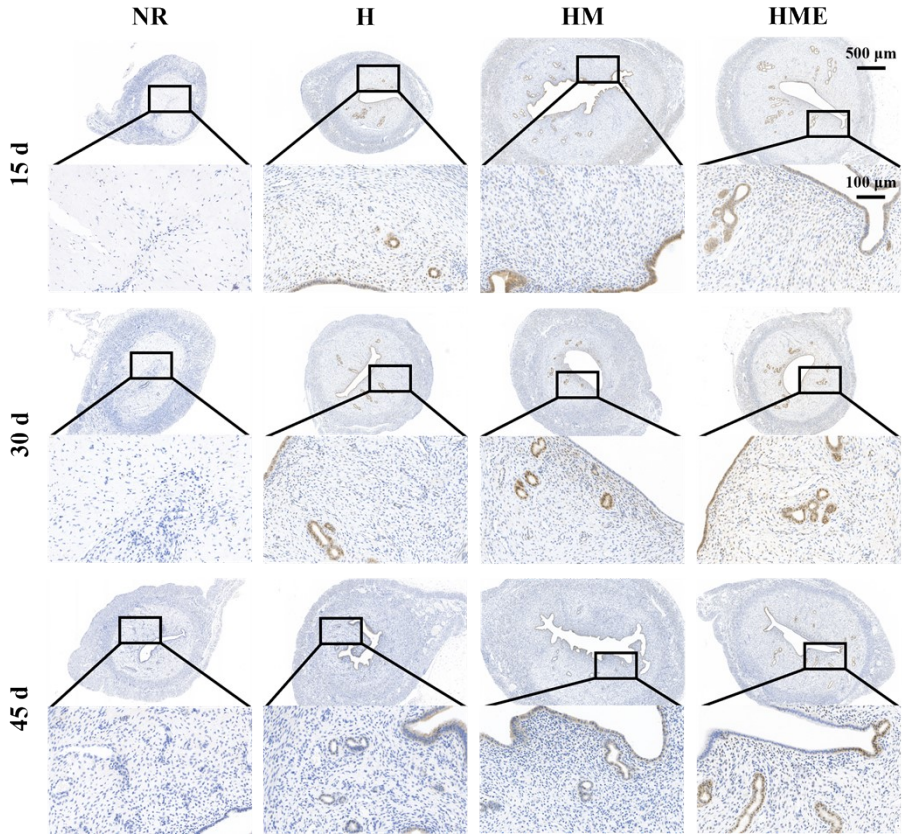

Fig. S12. Representative images of immunohistochemical staining of ER of uteri at 15 d, 30 d and 45 d after different treatments.